Recent numerical developments in scrape-off-layer global fluid simulations using the GBS code

S. Jolliet, F. Halpern, A. Mosetto, J. Loizu and P. Ricci

Ecole Polytechnique Fédérale de Lausanne (EPFL), Centre de Recherches en Physique des Plasmas, Association Euratom-Confédération Suisse, CH-1015 Lausanne, Switzerland

1. Introduction and Motivation

- Global 3D flux-driven fluid simulations of the SOL are presented using the GBS code [1]
- Interplay between the plasma outflow from the core, perpendicular transport and parallel losses at the limiter
- Field-aligned approach inadequate for X-point geometry as $q \to \infty$
- Several numerical schemes for the parallel gradient are studied

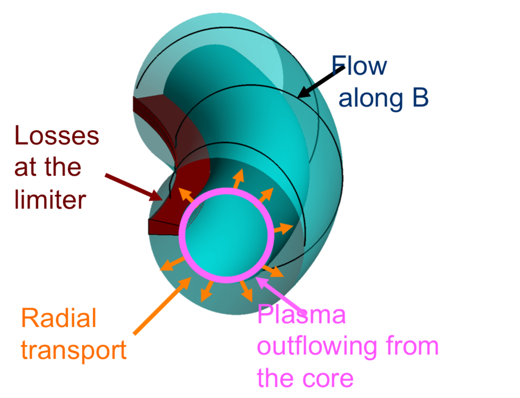

2. Simulation Model

- Drift-reduced Braginskii equations [2] with cold ion approximation $T_i = 0$

$$
\begin{aligned}
\frac{\partial n}{\partial t} &= -\frac{R_0}{B}[\phi, n] + \frac{2}{B}[C(p_e) - C(\phi)] - \nabla \cdot (n V_{\parallel e} \mathbf{b}_0) + \mathcal{D}_n(n) + S_n \\
\frac{\partial \omega}{\partial t} &= -\frac{R_0}{B}[\phi, \omega] - V_{\parallel i} \mathbf{b}_0 \cdot \nabla \omega + \frac{B^2}{n} \nabla \cdot (j_\parallel \mathbf{b}_0) + \frac{2B}{n} C(p_e) + \frac{B}{3n} C(G_i) + \mathcal{D}_\omega(\omega) \\
\frac{\partial \chi}{\partial t} &= -\frac{R_0}{B}[\phi, V_{\parallel e}] - V_{\parallel e} \mathbf{b} \cdot \nabla V_{\parallel e} + \frac{m_i}{m_e}\Big(\nu \frac{j_\parallel}{n} + \mathbf{b} \cdot \nabla \phi - \frac{1}{n}\mathbf{b} \cdot \nabla p_e - 0.71 \mathbf{b} \cdot \nabla T_e - \frac{2}{3n}\mathbf{b} \cdot \nabla G_e \\
&\quad + \frac{1}{n} G_e \nabla \cdot \mathbf{b}\Big) + \mathcal{D}_{V_{\parallel e}}(V_{\parallel e}) \\
\frac{\partial V_{\parallel i}}{\partial t} &= -\frac{R_0}{B}[\phi, V_{\parallel i}] - V_{\parallel i} \mathbf{b} \cdot \nabla V_{\parallel i} - \frac{1}{n}\mathbf{b} \cdot \nabla p_e - \frac{2}{3n}(\vec{b} \cdot \nabla) G_i - \frac{G_i}{n} \nabla \cdot \mathbf{b}_0 + \mathcal{D}_{V_{\parallel i}}(V_{\parallel i}) \\
\frac{\partial T_e}{\partial t} &= -\frac{R_0}{B}[\phi, T_e] - V_{\parallel e} \mathbf{b} \cdot \nabla T_e + \frac{4 T_e}{3B}\left[\frac{1}{n} C(p_e) + \frac{5}{2} C(T_e) - T_e C(\phi)\right] \\
&\quad + \frac{2 T_e}{3}\left[0.71 \nabla \cdot (j_\parallel \mathbf{b}_0) - \nabla \cdot (V_{\parallel e} \mathbf{b}_0)\right] + \mathcal{D}_{T_e}(T_e) + \mathcal{D}^{\parallel}_{T_e}(T_e) + S_{T_e} \\
\nabla_\perp^2 \phi &= \omega, \vec{\nabla}_\perp^2 \delta\psi = \frac{4\pi e}{c} n (V_{\parallel i} - V_{\parallel e}), \chi = V_{\parallel e} + \frac{m_i}{m_e}\frac{\beta}{2}\delta\psi \\
G_i &= -3\eta_{0i}\left[\frac{2}{3}\mathbf{b}_0 \cdot \nabla V_{\parallel i} - \frac{1}{3} V_{\parallel i} \nabla \cdot \mathbf{b}_0 + \frac{1}{B}\hat{C}(\phi)\right] \\
G_e &= -3\eta_{0e}\left[\frac{2}{3}\mathbf{b}_0 \cdot \nabla V_{\parallel e} - \frac{1}{3} V_{\parallel e} \nabla \cdot \mathbf{b}_0 + \frac{1}{B}\Big(-\frac{1}{n}\hat{C}(p_e) + \hat{C}(\phi) + \frac{2}{3} n C(p_e) - \frac{2}{3} C(\phi)\Big)\right] \\
\mathbf{b} \cdot \nabla A &= \mathbf{b}_0 \cdot \nabla A + \frac{\beta_e}{2}\frac{R_0}{B}[\delta\psi, A]
\end{aligned}
$$

- Circular concentric magnetic surfaces:
- $y = a\theta_*, x = r, z = R_0\varphi$ right-handed toric coordinate system
- Localized density and temperature sources around a given x_0
- Set of BC at the Magnetic Presheath Entrance where the Inertial Drift Approximation breaks down[3]
- Code applied to basic plasma physics devices [4]

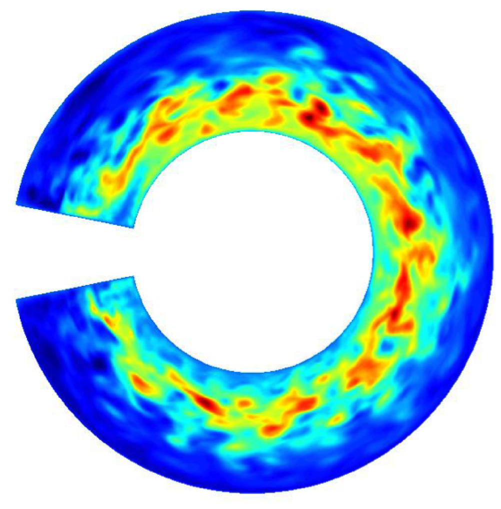

3. Numerics

- $(x, y, z) = (r, a\theta_*, R_0\varphi)$ coordinates, domain decomposition in x and z
- Second order centered finite difference scheme in the poloidal plane
- Anti-aliasing technique: filter toroidal modes for $n > N_z/4$
- Arakawa scheme for the Poisson bracket operator
- 4th order RK scheme for time advance
- $\phi, \delta\psi$ obtained from a linear system using one of LAPACK, Pardiso, MUMPS

Several options are considered for the parallel gradient operator:

- *fa scheme* (order 2):
  - stencil along the field line but $N_y/(qN_z)$ = integer.
  - Quadratic interpolation at the limiter plates in the toroidal direction
- *yz schemes* (order 2,4 or 6):
  - $\mathbf{b}_0 \cdot \nabla = \partial/\partial z + (a/q)\partial/\partial y$, centered finite differences in y and z
  - No constraint on the safety factor
  - One-sided derivatives at the limiter plates
- *yn schemes* (order 2,4 or 6):
  - $\mathbf{b}_0 \cdot \nabla = in + (a/q)\partial/\partial y$, centered finite differences in y and z
  - No constraint on the safety factor
  - One-sided derivatives at the limiter plates
- *mn scheme*:
  - $\mathbf{b}_0 \cdot \nabla = i(n + m/q)$, centered finite differences in y and z
  - No constraint on the safety factor
  - For poloidally-periodic systems only

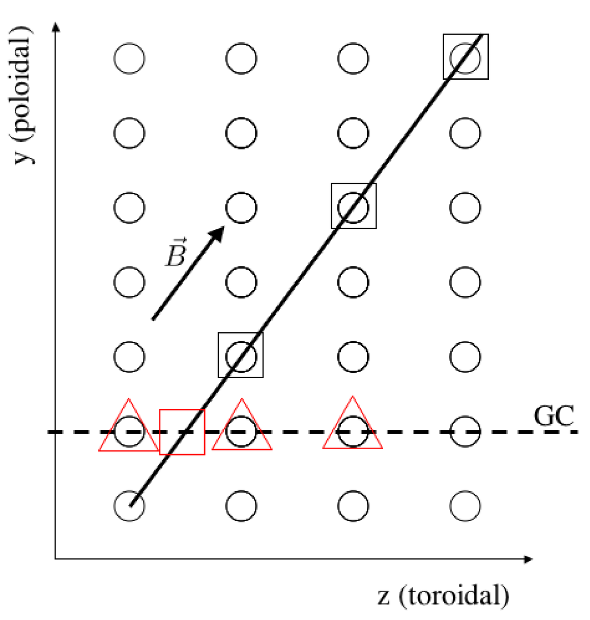

4. The Shear-Alfven wave test

- drift-reduced Braginskii equations can be reduced to the electrostatic shear Alfven wave with parallel diffusion:

$$
\begin{aligned}
\frac{\partial V_{\parallel e}}{\partial t} &= \frac{m_i}{m_e}\mathbf{b}_0 \cdot \nabla\phi + \frac{4\eta_{0e}}{3}(\mathbf{b}_0 \cdot \nabla)^2 V_{\parallel e} & (1) \\
\frac{\partial \nabla_\perp^2 \phi}{\partial t} &= -\nabla_\parallel V_{\parallel e} & (2)
\end{aligned}
$$

$\Rightarrow$ linearizing:

$$\omega = -i\gamma_D \pm \sqrt{\omega_0^2 - \gamma_D^2} \qquad (3)$$

with $\omega_0 = \sqrt{m_i/m_e} k_\parallel / k_\perp$ and $\gamma_D = 2\eta_{0e} k_\parallel^2 / 3$

- Parallel diffusion decreases the fundamental frequency ω_0 and damps the wave.
- A 2D (y,z) linear code has been written *using the same numerical algorithms as in GBS.*

[1] P. Ricci *et. al*, Plasma Phys. Control. Fusion 54, 124047 (2012)
[2] A. Zeiler *et. al*, Phys. Plasmas 4, 2134 (1997)
[3] J. Loizu *et. al*, Phys. Plasmas 19, 122307 (2012)
[4] P. Ricci and B. N. Rogers, Phys. Rev. Lett. 104, 145001 (2009) , Phys. Plasmas 16, 092307
[5] A. Mosetto *et. al*, Turbulent regimes in the tokamak scrape-off-layer, in press (Physics of plasmas)

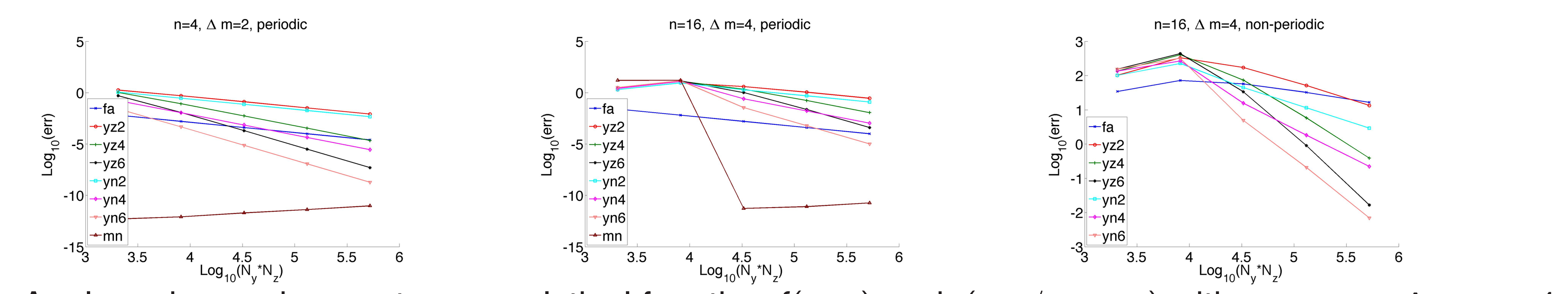

- Apply various schemes to an analytical function $f(y, z) = \sin(my/a - nz)$ with $m = nq + \Delta m, q = 4$.
- 4th order scheme with higher resolution accurate enough for low $k_\theta \rho_s$.
- 6th order scheme needed at high $k_\theta \rho_s$.
- Original *fa scheme* inaccurate at the boundary.

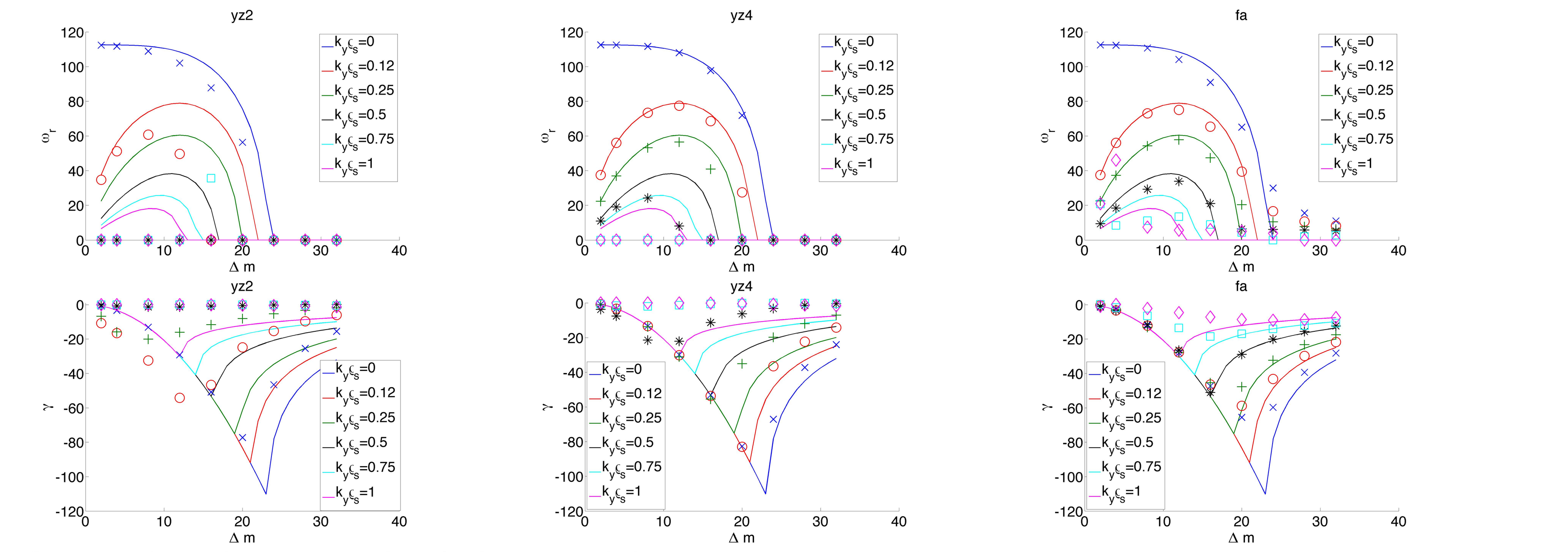

- Comparison between simulations and theory on a $(n, \Delta m)$ scan.
- $L_y = 200\rho_{s0}, q = 4, m_i/m_e = 200, \eta_{0e} = 5, N_y = 128, N_z = 32$ for all schemes except *fa scheme* for which $N_y = 256$.
- The *yz2 scheme* fails to reproduce the dispersion relation.
- The *yz4 scheme* and *fa scheme* is accurate up to $k_y \rho_s \cong 0.5$ for the given resolution while higher k_y modes are wiped out by numerical errors. The *fa scheme* gives a non-zero damping even at high k_y
- 6th order schemes, whether in real or Fourier space give similar results to 4th order schemes.
- The *mn scheme* recovers the dispersion relation perfectly.

5. GBS convergence tests

Electrostatic reference case: $L_y = 400, L_x = 100, N_x = 128, N_z = 32, N_y = 128, \Delta t = 6 \cdot 10^{-5} R_0/c_s, q = 4, \hat{s} = 0, m_i/m_e = 200, \nu = 0.1 c_s/R_0$

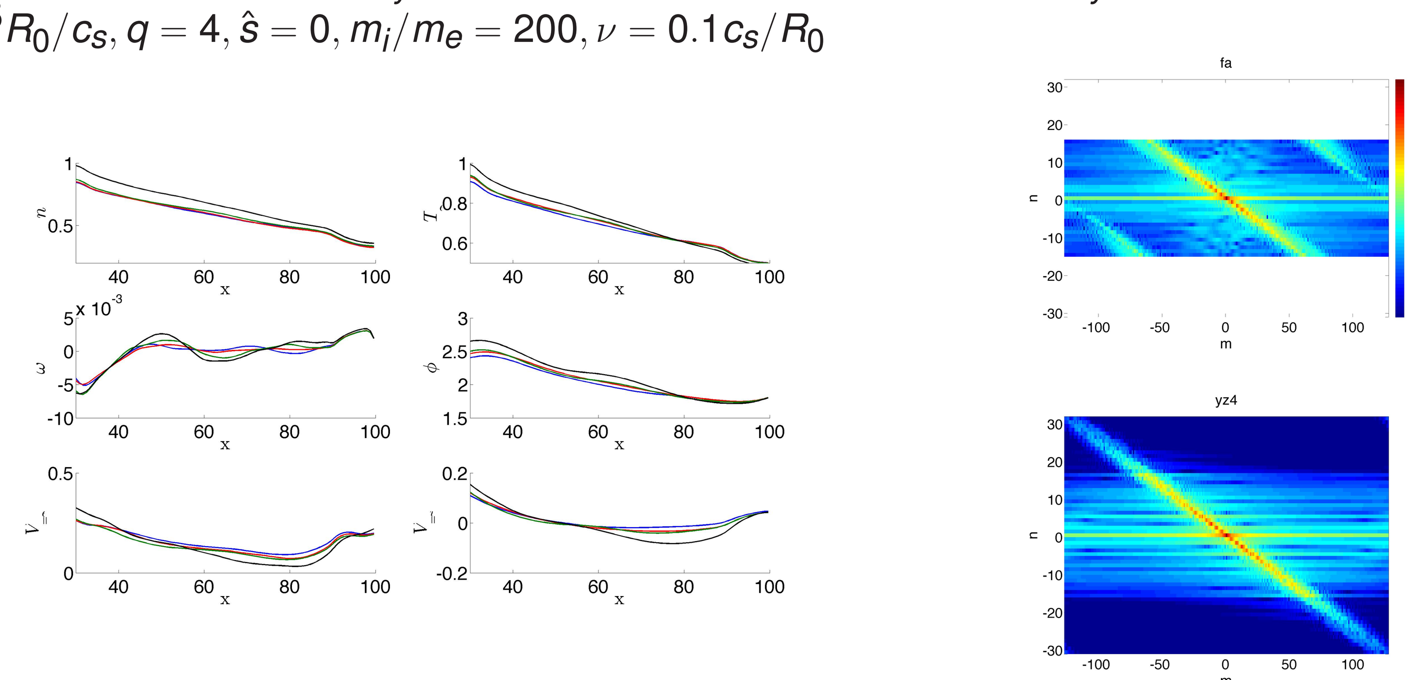

- Legend: *fa*, $N_y = 256$; *yz4*, $N_y = 256$; *yz4*, $N_y = 128$; *yz4*, $N_y = 64$
- By doubling the toroidal resolution and filtering toroidal modes one recovers the same steady-state.
- A poloidal resolution of $N_y \cong qN_z$ is sufficient to converge the results.
- The filtering procedure is efficient to prevent aliasing.
- *yn* scheme more costly - it will be implemented in the future.

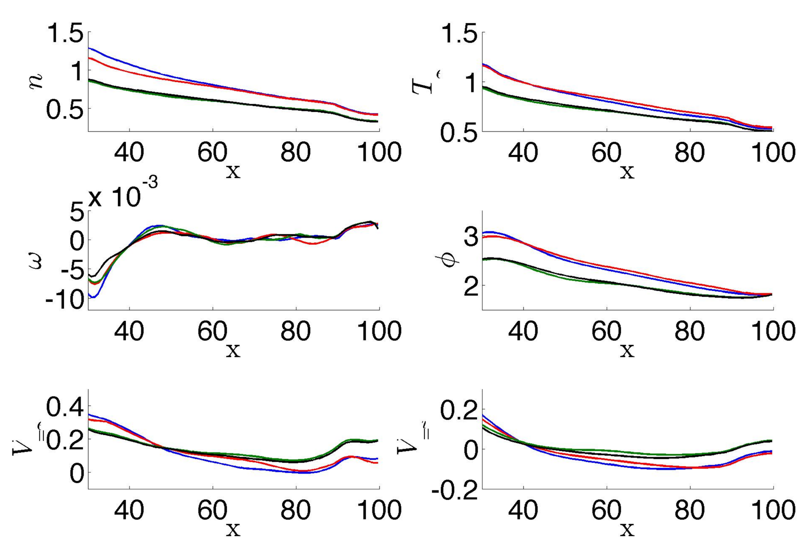

- N_z scan at fixed $N_y = 128$, filter out modes outside $[-N_z/4 : N_z/4]$ using the *yz4* scheme.
- Filtering procedure kills high-frequency shear-Alfven waves.
- Legend: $N_z = 16$; $N_z = 32$; $N_z = 64$; $N_z = 128$
- $N_z = 64$ sufficient for convergence.

5. GBS nonlinear simulations

- A safety factor profile with constant shear is introduced in GBS.
- The *yz4* scheme is used with $N_y = 128$, $N_z = 64$ and the filtering procedure.
- Eddy structure consistent with q-profile.
- Turbulence aligned with the magnetic field line.
- $R_0/L_{pe} = 21.7, 9.1, 6.5$ for $\hat{s} = -1, 0, 1$. Strong stabilization of RBMs at negative shear and destabilization at low positive magnetic shear has been observed in GBS local simulations[5].

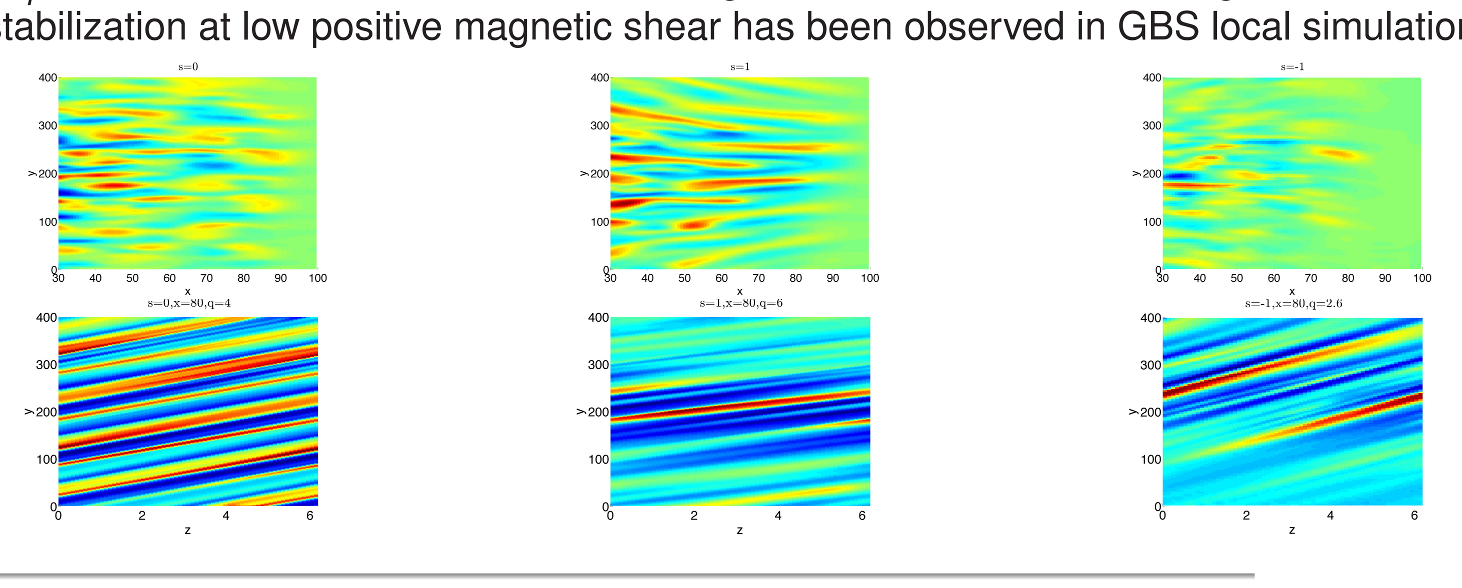

6. Conclusion

- The shear-Alfven wave problem is an efficient testbed for parallel gradient schemes
- *yz4* scheme with double toroidal resolution and filtering procedure recovers the field-aligned results
- First GBS simulations with global q profile show promising results

sebastien.jolliet@epfl.ch

23rd International Conference on Numerical Simulation of Plasma